# Cronfa - Swansea University Open Access Repository

_____

This is an author produced version of a paper published in :
*Marine Geology*

_____

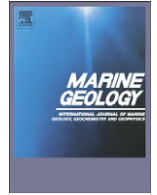Cronfa URL for this paper:

http://cronfa.swan.ac.uk/Record/cronfa25976

_____

_____

# Numerical modelling of storm and surge events on offshore sandbanks

I. Fairley *, I. Masters, H. Karunarathna

*College of Engineering, Swansea University, Swansea, United Kingdom*

## ARTICLE INFO

## ABSTRACT

This contribution uses a 3 dimensional coastal area numerical model, DHI's MIKE3, to simulate the impact of storm and surge events on offshore sandbanks. Three offshore sandbanks in the Bristol Channel are considered due to the region's sensitivity to anthropogenic pressures and the gradients in wave and tidal forcing in the area. Two extreme storm and surge events are simulated: one co-incident with spring tide and the other with neap tide. Reference simulations of astronomical tidal forcing only are also presented. It is shown that for the two sandbanks with greater wave exposure, storm conditions can provide a mechanism for the maintenance of crest position. For these cases, bed level changes over the crest are in the opposite direction compared to astronomically forced change. For the least wave exposed bank, both wave and tide only cases exhibit similar patterns of bed level change. Volumetric changes under astronomical forcing are shown to vary with changing maximum tidal current. Accretion occurs over a neap tidal cycle for all three sandbanks and as maximum tidal current increases the amount of accretion increases; however, over a spring tidal cycle accretion is observed for the less tidally dominated site but increasing maximum tidal current leads to reduced accretion and then erosion for the most tidally dominated bank. Volumetric changes under storm conditions are related to sandbank morphology and setting rather than relative wave exposure. The two single banks closely tied to headlands show similar magnitude of percentage volumetric change despite being at the two extremes of wave exposure and greater erosion occurs over the neap tide event. The sandbank that has associated secondary banks shows lesser percentage change and greater erosion over the spring tide event.

© 2015 The Authors. Published by Elsevier B.V. This is an open access article under the CC BY license (http://creativecommons.org/licenses/by/4.0/).

## 1. Introduction

Offshore sandbanks have societal importance as a form of natural coastal protection (Dolphin et al., 2007), a source of aggregates (Idier et al., 2010; Phillips, 2008; Van Lancker et al., 2010), sites for offshore wind installations and an important marine habitat (Atalah et al., 2013). Sandbanks can be important fish nursery areas (Neill, 2008) and the ecosystem function of offshore sandbanks mean that they are candidate SACs under the EU habitats directive (Atalah et al., 2013). Work conducted on sandbanks around the Welsh Coast has shown that the biological assemblages of sandbanks are distinct from other nearshore areas (Kaiser et al., 2004). The coastal protection function of offshore sandbanks is primarily related to wave dissipation over sandbanks leading to reduced wave energy on the lee side. Wave conditions have been linked to water depth over a sandbank (Park and Vincent, 2007). Model studies have shown that inshore wave height can vary by 0.5 m depending on tidal level (Coughlan et al., 2007). Sediment transport links between beaches and sandbanks have also been suggested (Dolphin et al., 2007; Phillips, 2008).

A significant body of work has investigated the dynamics of offshore sandbanks both via numerical modelling and experimental studies.

Work has focussed on the role of tidal currents in bank formation and maintenance (Berthot and Pattiaratchi, 2005, 2006; Collins et al., 1995; Neill, 2008; Pattiaratchi and Collins, 1987), short term tidally induced sediment dynamics (Bastos et al., 2004), long term morphological (Horrillo-Caraballo and Reeve, 2008; Reeve et al., 2001) and volumetric changes (Lewis et al., 2014), sediment transport pathways around sandbank systems (Schmitt and Mitchell, 2014), between the nearshore and sandbanks (Dolphin et al., 2007) and on the behaviour and morphology of associated bedforms (Bastos et al., 2002; Scmitt et al., 2007). More recently, work has been conducted on the role of wave driven transport, however, there is not a large body of work focussing on wave or storm driven processes (Giardino et al., 2010). Measurement campaigns have shown that not only can storms reduce crest elevations but that grain size distributions can be affected with winnowing of material on the crest and deposition of finer particles in more sheltered areas (Houthuys et al., 1994). It has been demonstrated that waves can both magnify the quantity and alter the direction of sediment transport around sandbanks (Pattiaratchi and Collins, 1988). This means that there is the potential for storm events to have a role in the long term maintenance of sandbanks. However, there is some disagreement on the importance of storm impacts on sandbank morphology given their episodic nature. Measured data on sediment concentration on the Middelkerke Bank showed that over a 40 day period the majority of transport occurred during a few hours where large waves and strong

* Corresponding author.
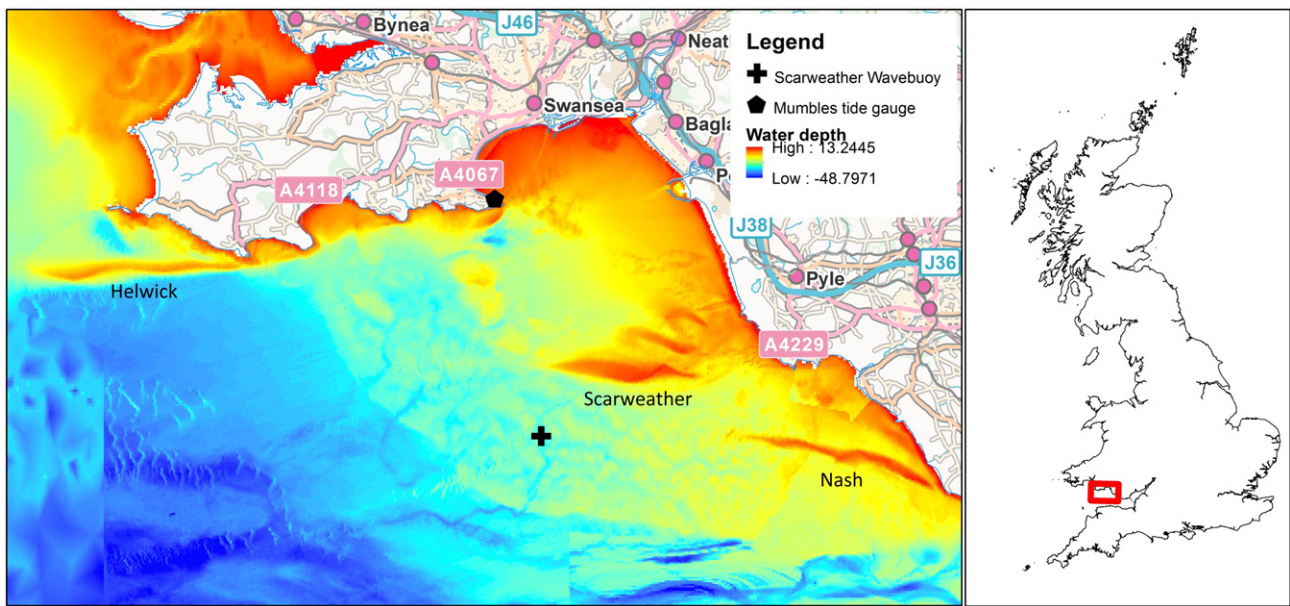*E-mail address:* i.a.fairley@swansea.ac.uk (I. Fairley).

**Fig. 1.** A map showing the bathymetry of Swansea Bay with the Mumbles tide gauge, Scarweather Sands wave buoy and studied sandbanks marked (main panel) and a map of the United Kingdom showing the location of Swansea Bay (right panel).

current combined (Vincent et al., 1998). Conversely, other researchers hold that the infrequent nature of storms mean they are not important compared to the background stirring effect of low energy waves (van de Meene and van Rijn, 2000).

There is increasing pressure on the Bristol Channel environment both from industrial developments and climate change. Significant renewable energy infrastructure projects have been proposed in the Bristol Channel region such as tidal stream turbines (Ahmadian et al., 2012; Ahmadian and Falconer, 2012), the Severn Barrage (Xia et al., 2010), the Atlantic Array windfarm and various tidal energy lagoons (TLSB, 2014). These have the potential to impact wave (Fairley et al., 2014) and hydrodynamic (Xia et al., 2010) conditions in the area. Aggregate dredging in the region has been reported to remove $0.5 \times 10^6$ m$^3$ from the Nash sandbank every year (Lewis et al., 2014). Equally, climate change is predicted to lead to sea level rise in the Irish Sea of 0.47 m in the 21st Century (Olbert et al., 2012). Various studies have predicted that storm surges are likely to increase in both frequency and severity (Lowe and Gregory, 2005; Lowe et al., 2001; Wang et al., 2008) and wave climate may also become stormier via anthropogenic climate change.

These factors are not specific to the Bristol Channel; growing world population and increased utilisation of the coastal zone mean appropriate management strategies are essential worldwide (Dafforn et al., 2015) and evidently climate change is a global phenomenon. The increased capacity for coastal change and increased recognition that preservation of the current value and function of habitats is important means that it is crucial to develop understanding to facilitate better management. Developing understanding of storm event dynamics is particularly important due to the magnitude of change that can occur under such conditions and the predictions that extreme storms may increase in frequency (Lionello et al., 2008).

This paper specifically addresses the impact of storm and surge events on the morphology of offshore sandbanks in the Bristol Channel using the numerical model MIKE3FM from the Danish hydraulic institute. Three sandbanks are modelled: the Helwick Bank, Scarweather Sands and the Nash Bank (Fig. 1). Two storm events with similar parameters ($H_s$, $T_p$, surge), one co-incident with spring tide and one co-incident with neap tide are investigated to elucidate the difference between the impacts of storms impacting at different stages of the spring–neap cycle. Simulations consisting only of astronomical forcing are also presented. This provides new understanding of the differences in morphodynamics between storm wave and tidal forcing.

## 2. Study site

This study focusses on three sandbanks in the northern Bristol Channel, from west to east these are: Helwick, Scarweather and Nash (Fig. 1). All three sandbanks are around 10 km long with heights of about 20 m above the surrounding seabed. The Helwick and Nash Banks are single sandbanks, while the Scarweather Bank has two smaller associated
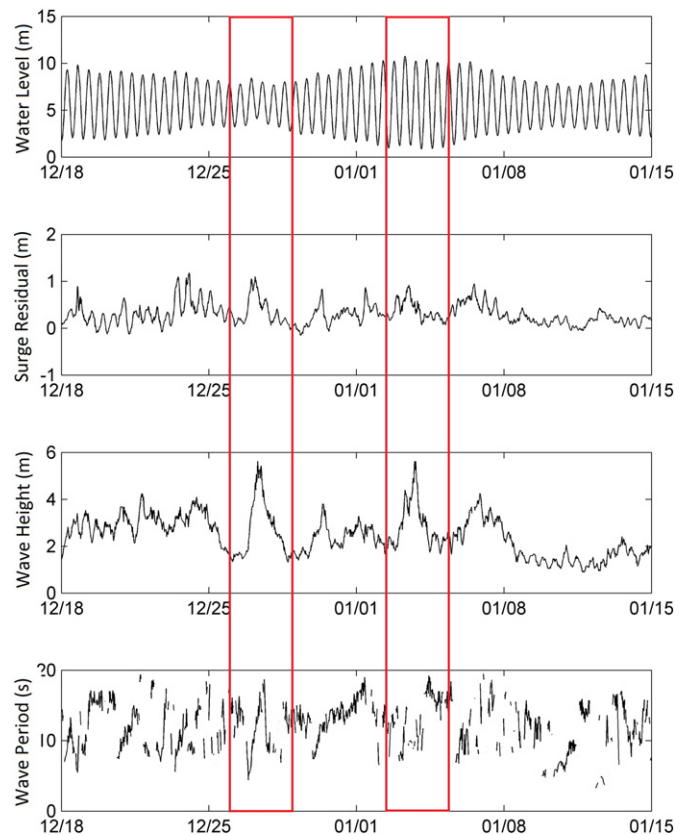


**Fig. 2.** Plots of wave and hydrodynamic parameters for the time period of interest with the two storms ringed in red.
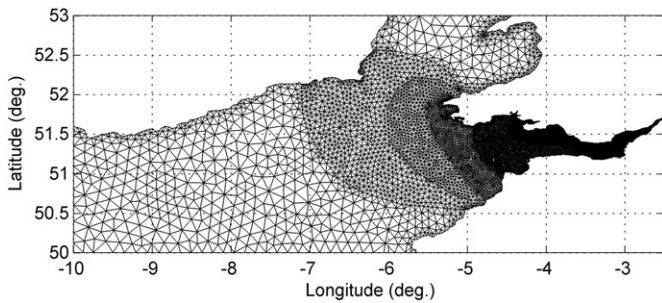
Fig. 3. The model domain and mesh used for the hydrodynamic and sediment transport simulations (mesh A).



Fig. 5. BGS sample points (○) and the grain size interpolated to the model mesh (colour shading).

banks further north. The banks are all headland associated sandbanks. The Bristol Channel is an energetic megatidal environment: the mean spring tidal range at the nearest tide gauge (Mumbles) is 8.5 m. The difference in range between springs and neaps is substantial with the mean neap range only 4 m (NTSLF, 2014). There is also a strong spring neap variation in residual current speeds (Uncles, 2010). Tidal currents in the region can cause modulation of wave heights in the area (Fairley et al., 2014). Therefore one can expect the timing of storm events through the spring neap cycle to be important.

The area is open to large swell and wind waves from the Atlantic: fetch lengths exceed 6500 km from the west and south west which coincide with the direction of the prevailing winds and approach of low pressure systems. Correspondingly, prevailing wave directions are also from the west to south west (HSE, 2001). It has been reported that in the outer Bristol Channel, 75 km to the west of the studied area, significant wave height exceeds 3 m for 10% of the time and the 50 year return period wave is 18 m (Draper, 1991). Surges are common in the region given the location and orientation of the funnel-shaped Bristol Channel. Based on a numerical modelling study it has been reported that surge levels in the general study region can exceed 1.5 m for a 50 year return period, with associated surge currents of 0.2 m s$^{-1}$ (Flather, 1987).

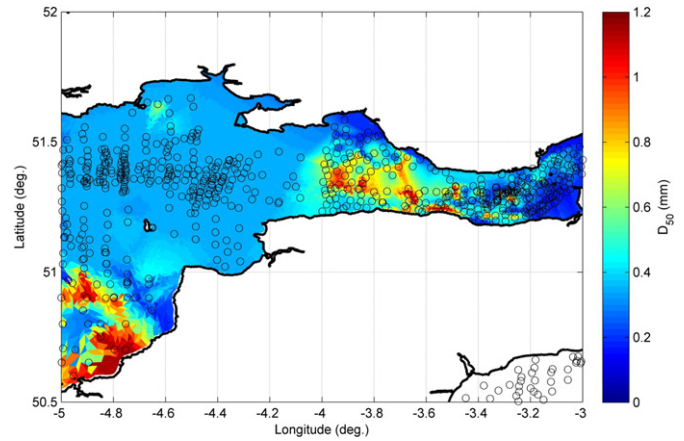A range of previous work has investigated the dynamics of the sandbanks in the region. Past work has investigated the formation and maintenance of the banks (Pattiaratchi and Collins, 1987), sediment transport in the vicinity (Pattiaratchi and Collins, 1988), shape of bed forms on the banks (Schmitt and Mitchell, 2014) and volumetric changes (Lewis et al., 2014). It has been shown that the sand making up the Helwick Bank was deposited during the last glaciation and there is little input from modern rivers (Schmitt and Mitchell, 2014).

Pattiaratchi and Collins (1987, 1988) have previously investigated the Scarweather Sands Bank. They describe Scarweather as being at the distal end of a sediment transport pathway, with the bank maintained by tidal currents and with sediment removed from the crest via wave action (Pattiaratchi and Collins, 1988). In the region of Scarweather Sands, the presence of waves increases the rate of sediment transport. Eastward (up-channel) transport is increased under wave action, and in some locations direction of sediment transport is changed or reversed by the presence of waves (Pattiaratchi and Collins, 1988). Pattiaratchi and Collins (1987) suggest Scarweather Sands is in equilibrium with the current hydrodynamic regime based on measurements of currents, bathymetry and sediment properties. They infer from asymmetry in the
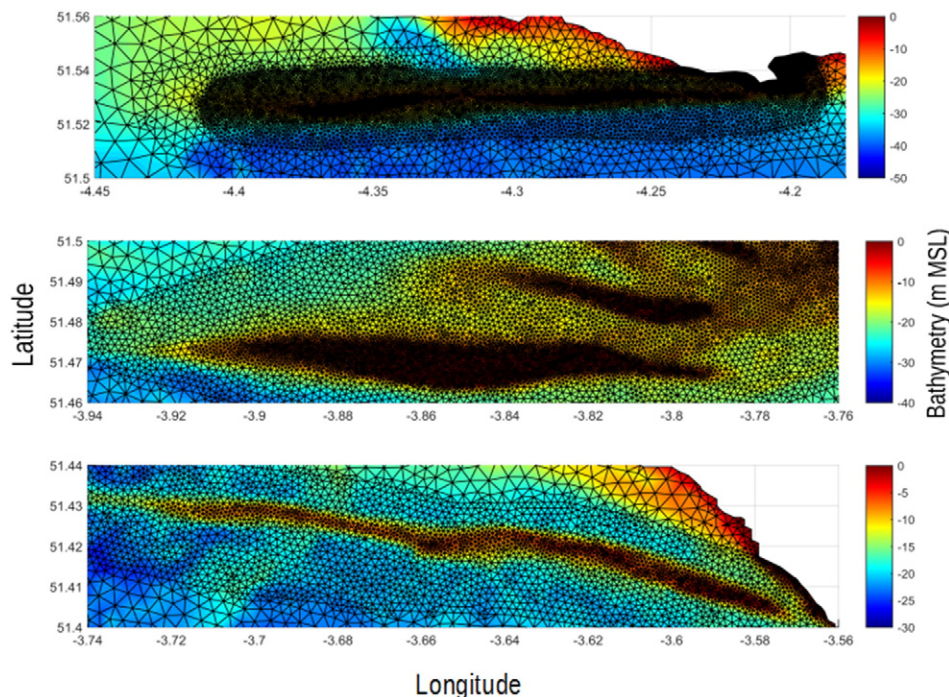


Fig. 4. Close-ups of mesh A over the sandbank areas for the three sandbanks, from top to bottom: Helwick, Scarweather and Nash.
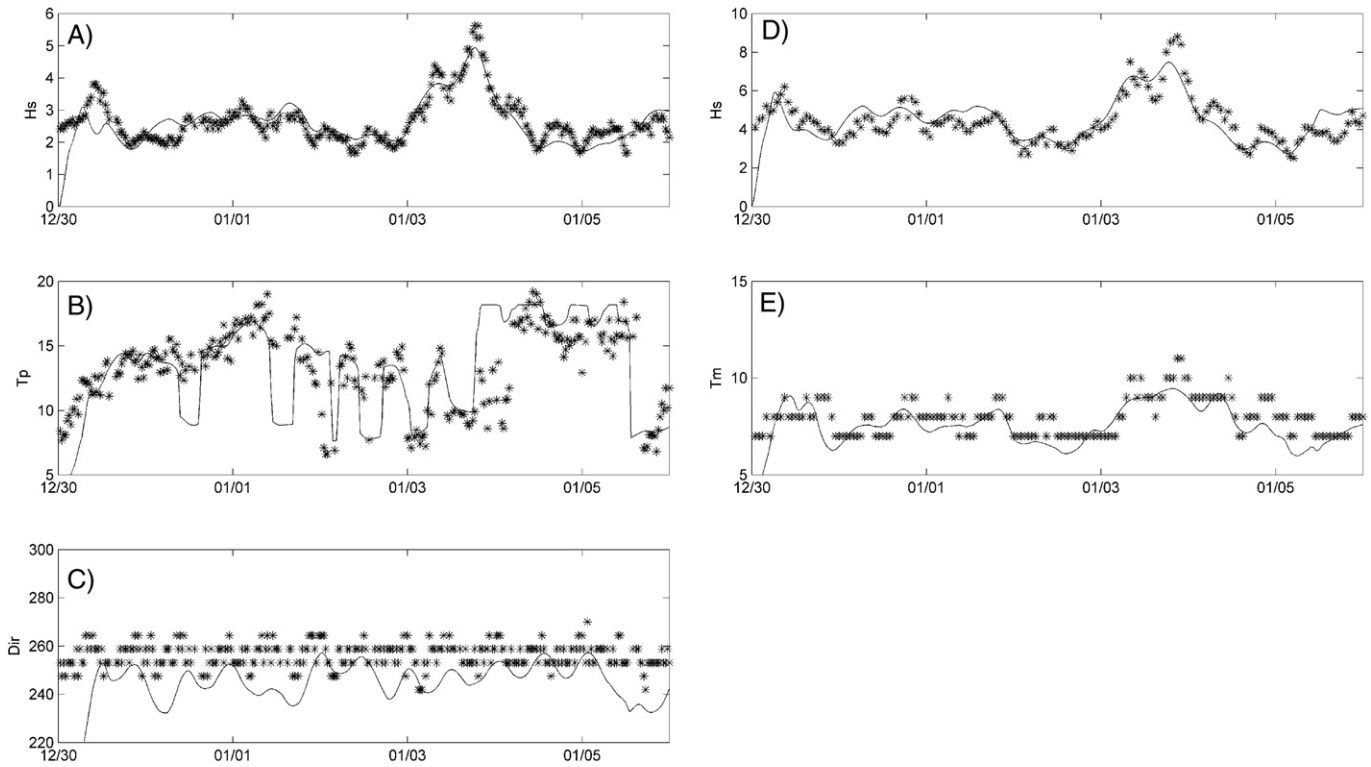
Fig. 6. A comparison of modelled (—) and measured (*) wave conditions: A) wave height at Scarweather; B) peak period at Scarweather; C) direction at Scarweather; D) wave height at Turbot Bank; and E) mean period at Turbot Bank.

cross-bank profile that the western half is dominated by currents on the southern flank and the eastern half by currents on the northern flank. They suggest that the broader western end compared to the eastern end is due to wave action from the South West. Sand transport pathways inferred from mega-ripples and sandwaves suggest a clockwise sediment transport pathway around the bank. Residual current patterns are also in a clockwise direction around the bank. Over the crest there is a reversing flow on flood and ebb tides which is at an oblique angle to the longitudinal axis of the sandbank.

Lewis et al. (2014) investigated the change in volumes of the Nash and Helwick Banks between 1991 and 2002 using bathymetric survey data. It is suggested that Helwick can be considered a wave dominated bank and Nash a tidally dominated bank. It was found that both sandbanks reduced in volume at a rate greater than the rate extracted by the aggregates industry. They found that volume change correlated well with the 'effective' wave climate, the duration in which wave driven currents were greater than the critical threshold of motion. The interannual variability is attributed to the number of storms each year. Increased number of storm events lead to an increase in volume at the Nash Bank and a reduction in volume at Helwick Bank. It is postulated that this is due to the reduction from West to East in wave height for a given storm along with an increase from West to East in tidal velocity. 2D simulations of morphological change over a cross-bank profile of Helwick Bank showed that morphological changes that occur at the peak of a storm are also dependent on the water levels at that time.

## 3. Time period of interest

This contribution focusses on the impact of two storms from the exceptionally stormy winter of 2013/14. The neap tide storm peaked at 27/12/2013 07:30 and the spring tide storm peaked at 03/01/15 19:30. The hydrodynamic conditions during this period are shown in Fig. 2 with the two storm events highlighted. Tidal data is taken from the Mumbles tide gauge and wave data from the Scarweather Sands wave buoy (for locations see Fig. 1). For both cases the peak significant wave height reaches 5.6 m.

In order to put these two storms into context, the entire record of the Scarweather Sands wave buoy (September 2005–November 2014) was analysed for storm events. Storms were taken to be conditions when wave heights exceed 2.7 m. The threshold value (2.7 m) is equal to the mean wave height plus twice the standard deviation in the wave record. No storm wave height threshold had previously been defined for the wave buoy used and visually this value gave a reasonable seasonal spread of storm events. A peak finding routine was then used to find peak wave heights over this value, a minimum separation of 36 h between peaks was stipulated to ensure each peak was an independent storm event. Over the 9 year record 338 storms meeting these criteria were identified, and when these were ordered by wave height, the two analysed storms were ranked 6 and 7. The same analysis was conducted for a 22-year record from the Turbot Bank buoy, situated further west (51.603 N, 5.1 W), and showed that the two storms were ranked 12 and 14 out of 598. These rankings show not only that the

**Table 1**
$r^2$ and root mean square errors (RMSE) for wave parameters at the two sites at spring and neap tides.

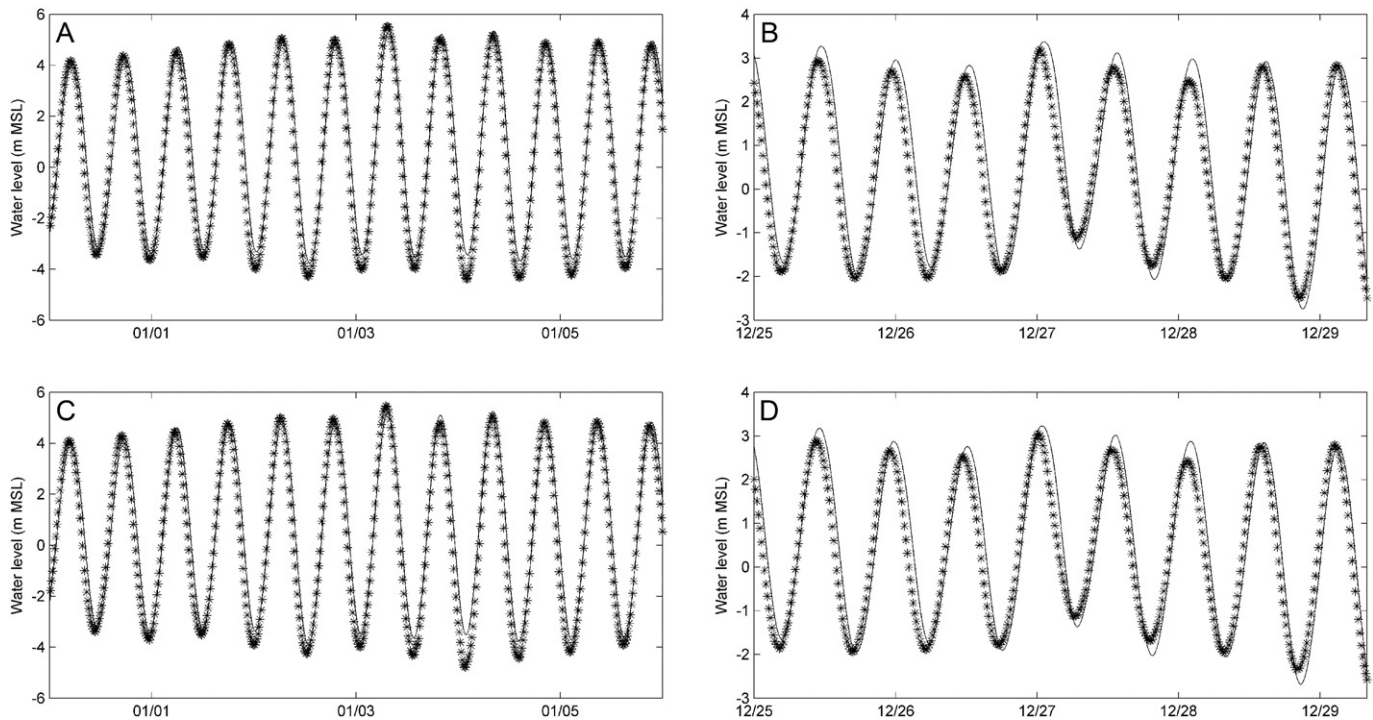| | Scarweather Hs | | Scarweather Tp | | Scarweather Dir | | Turbot Bank Hs | | Turbot Bank Tm | |
|---|---|---|---|---|---|---|---|---|---|---|
| | Spring | Neap | Spring | Neap | Spring | Neap | Spring | Neap | Spring | Neap |
| $r^2$ | 0.79 | 0.9 | 0.29 | 0.2 | 0.07 | 0.17 | 0.6 | 0.90 | 0.41 | 0.52 |
| RMSE | 0.33 | 0.33 | 3.1 | 3.4 | 12 | 12 | 0.78 | 0.6 | 1 | 1 |

Fig. 7. Measured and modelled water levels for A) Mumbles spring tide, B)Mumbles neap tide, C) Ilfracombe spring tide and D) Ilfracombe neap tide.

two storms are in the upper 2% of measured storm events but that they are very similar in their peak wave height ranking with only the time relative to the tidal cycle different.

## 4. Methodology

In this section the numerical model used, MIKE3, is briefly outlined before modelling strategy, model domain, forcing, set up and validation are described.

MIKE3 is a commercially available 3 dimensional coastal area model with a range of modules for various applications. In this study three modules are utilised: hydrodynamic; spectral waves and sand transport. MIKE was selected for the availability of an unstructured mesh implementation for all modules, reliable coupling between modules and due to its well-regarded reputation. Unstructured meshes have the advantage that complex shorelines and bathymetries can be well resolved in regions of interest while computational power can be conserved by lowering resolution away from the study area. Optimisation of computer resources is of paramount practical importance when conducting coupled modelling on a desktop PC. Equally good representation of the shoreline and bathymetry around headland associated sandbanks improves modelling of the residual circulation.

The hydrodynamic module solves the 3 dimensional incompressible Reynolds averaged Navier–Stokes equations with the assumptions of Bousinesq and hydrostatic pressure (DHI, 2012a, 2012b). In this study the higher order solution technique was used for both space and time. Default parameterisations were used for eddy viscosity with a Smagorinsky formulation (Smagorisky, 1963) for horizontal eddy viscosity and a log law formulation for vertical eddy viscosity. Bed resistance was specified as roughness height with a value of 0.1 m applied in the outer region and a value of 0.05 m in the area of interest. Lower values of bed resistance were tested but led to model instabilities. Model instabilities were initially observed in the intertidal region of Swansea Bay; this was due to the wide, shallow gradient, intertidal region leading to isolated wet elements and very shallow wet elements. Past experience has shown that increasing flooding and wetting depths removes this source of instability and hence flooding and wetting

depths were increased from the default values to 0.15 m and 0.3 m respectively which rectified the error.

The spectral wave module simulates wave transformation over the model domain based on the wave action conservation equation (Sorenson et al., 2004). A fully spectral formulation with an instationary time formulation was used. Default settings were used for most parameters: frequency discretisation was logarithmic and directional discretisation a 360° rose with 24 directions; white-capping, diffraction and quadratic wave–wave interactions were included but triad interactions were omitted.

Within MIKE3 different sediment transport formulae are used depending on whether waves are present in the simulation or not. For pure current cases the theories of Van Rijn (1984a, 1984b) for bed load and suspended load are used. For the cases with waves present, a quasi 3-D approach is utilised to compute total load transport based on a previously computed look-up table. To compute the look-up table, total load is calculated for a range of wave and current conditions by calculating bed-load using Englund and Fredsoe (1976) and suspended load using Fredsoe et al. (1985).

### 4.1. Modelling strategy

Four key tests were run for this study: storm and surge over a spring tide; storm and surge over a neap tide; and reference tests over the same time period with solely astronomical tidal forcing. The neap tide simulation started at 24/12/13 00:00:00 and ran until 31/12/13 00:00:00. Results are considered for the two tidal cycles over the peak of the storm between 26/12/13 18:20 and 27/12/13 19:50. The spring tide simulation started at 30/12/13 00:00:00 and ran until 04/01/14

**Table 2**
$r^2$ and root mean square errors (RMSE) for water level at the two sites at spring and neap tides.

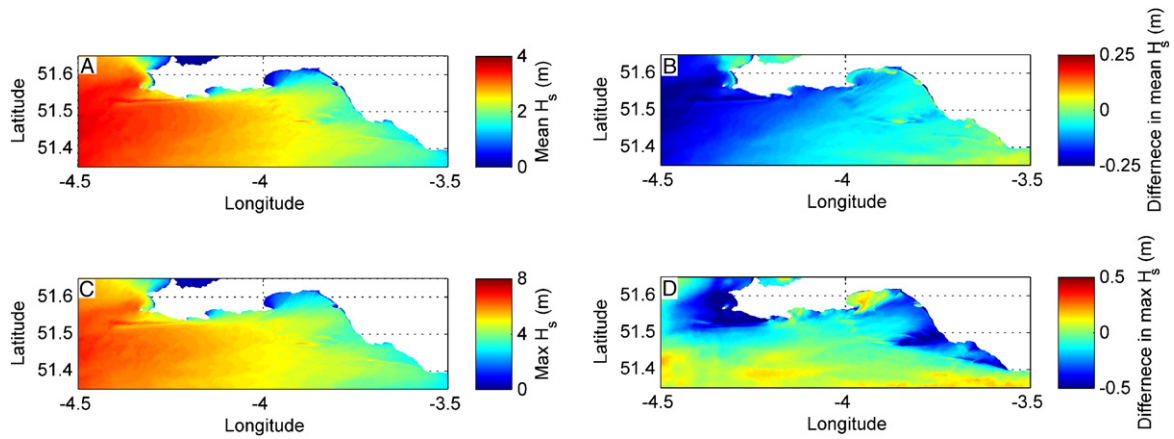|  | Mumbles neap | Mumbles spring | Ilfracombe neap | Ilfracombe spring |
|---|---|---|---|---|
| $r^2$ | 0.9 | 0.96 | 0.9 | 0.96 |
| RMSE | 0.6 | 0.7 | 0.6 | 0.7 |

**Fig. 8.** A) Mean wave heights for the neap tide event, B) difference in mean wave height between the neap and spring storm event, C) maximum wave height for the neap storm event, and D) difference in maximum wave height between the neap and spring storm event.

21:40:00. For the spring tide test results are considered for the two tidal cycles between 03/01/14 01:20:00 and 04/01/14 02:00:00. Bed morphology was held constant until the start of the results period (onset of storm) to ensure that for comparison of changes between tests all the simulations had the same starting bed level.

For the astronomical forcing tests, only the sediment transport and hydrodynamic module was used. These were run in a fully coupled mode. For the simulations with waves present, the hydrodynamic and sediment transport models were run fully coupled with offline forcing from a previously run wave simulation. The reason for this approach was that the density of mesh required to produce sufficiently high resolution results for morphological change (mesh A) was such that the computational time to run a wave simulation was prohibitively high. Instead a coarser mesh (mesh B) was used to simulate wave conditions. The procedure used was:

• Run hydrodynamic simulation on mesh A
• Run spectral wave simulation on mesh B with tidal current and level forcing from the previous hydrodynamic run
• Re-run the hydrodynamic simulation on mesh A, coupled with the sediment transport module and with forcing from the spectral wave model results.

The major drawback of such an approach is that waves are not influenced by the changing bathymetry over the model run. However, since a fully coupled run was predicted to take several thousand hours on the

available desktop workstation, this approach is deemed appropriate for pragmatic reasons.

Cohesive sediment transport was neglected in this study despite there being a substantial quantity of finer sediment in the region and high suspended loads under certain conditions. This was in part due to the computational expense and in part due to the lack of available data on cohesive and suspended sediment. Equally, cohesive sediment is less relevant to the offshore sandbanks than to other environments in the region.

### 4.2. Model domain and meshes

The model domain covers from 10°W to 2°W and from 50°N to 53°N, thereby encapsulating the Bristol Channel, the southern Irish Sea and the Celtic Sea. Vertical resolution is based on seven sigma layers. Horizontal resolution is catered for with a flexible unstructured mesh: for mesh A the element area ranged from a value of $0.015°^2$ for the coarsest area to $2 \times 10^{-6°2}$ in the sandbank areas. This equates to node separation distances of between 19 km in the outer region and 200 m in the finest areas. Variation in mesh area was kept well below the limit of a factor of 10 between adjacent regions that is suggested by DHI for stable and accurate model runs. The sandbank regions were then further refined based on water depth. Fig. 3 shows the entire mesh and Fig. 4 shows a close-up of mesh A over the three sandbanks. Mesh B used the same boundaries and bathymetry as mesh A. The specified mesh sizes were also kept the same, the only difference was that there was no further depth based refinements in the sandbank regions.
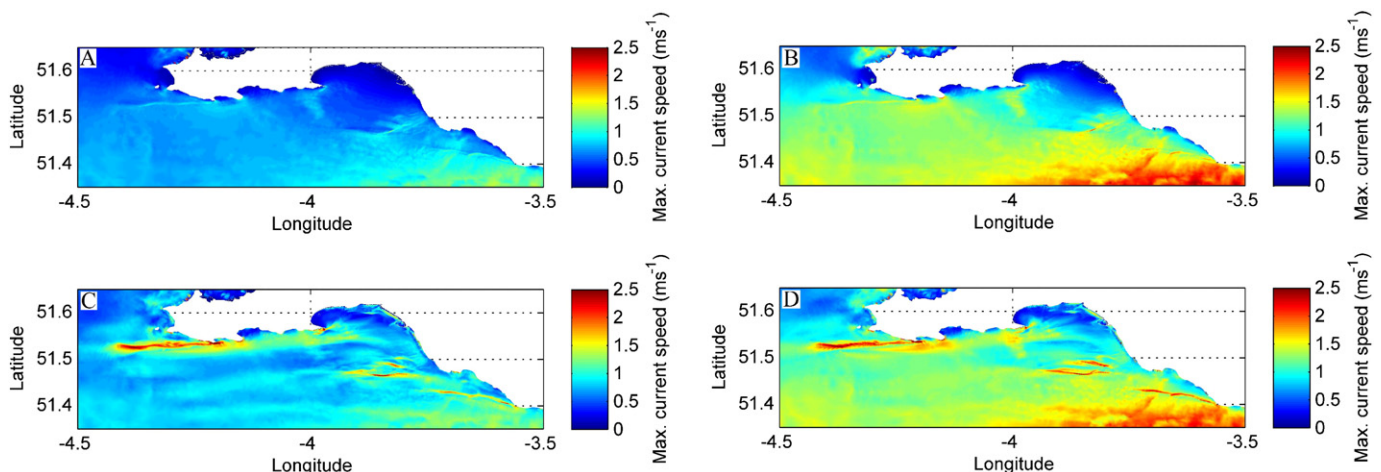


**Fig. 9.** Maximum current speeds for A) neap astronomical tide, B) spring astronomical tide, C) neap storm and surge, and D) spring storm and surge.

Two sources of bathymetry were used in this study: for the wider area where no finer bathymetry data was available GEBCO (Hall, 2006) gridded bathymetry was used; for the area of interest bathymetry was downloaded from the UKHO inspire portal (UKHO, 2014). The GEBCO bathymetry is referenced to mean sea level. The data from the UKHO inspire portal is referenced to chart datum and therefore the UK vertical offshore reference framework (VORF) (Iliffe et al., 2013) was used to translate these data to mean sea level. VORF (Iliffe et al., 2013) provides a set of surfaces that allows for translation between different datums (MSL, LAT, and CD) around the UK coast.

### 4.3. Model forcing and sediment data

The reference models of astronomical tides alone are forced at the open boundaries with water level from DHI's global tidal atlas (Anderson, 1995, 1999). Based on comparison with readings from 102 tide gauges, the model shows RMS differences of between 1.1 cm and 2.51 cm for the $O_1$, $K_1$, $S_2$, and $M_2$ constituents (Anderson, 1995). Coriolis forcing and tidal potential are applied across the model domain (DHI, 2012a, 2012b).

For the storm and surge models: atmospheric forcing (wind and pressure) from the ECWMF ERA-interim dataset (Dee et al., 2011) is applied across the domain; wave forcing for the offshore boundaries is also taken from the ERA-interim dataset. ERA-interim is a global reanalysis dataset which uses sequential data assimilation. The methodology and outputs have been rigorously evaluated (Dee et al., 2011). The data assimilation uses satellite scatterometers (ERS-1, ERS-2, Quikscat) to provide surface wind vector fields over oceanic waters, ocean wave predictions are constrained using satellite altimetry wave height observations from ENVISAT, JASON-1 and JASON-2 (Dee et al., 2011). ERA-interim wave parameters and 10 m wind speeds are reported to show a marked improvement relative to the previous ERA-40 reanalysis, and the overall quality of wave parameters in the ERA-interim dataset is equal to the operational analysis of 2005 (Dee et al., 2011). Water levels at the boundaries are taken from a North Atlantic model which was run in MIKE with tidal boundaries from DHI's global tidal atlas and atmospheric forcing from the ECMWF ERA interim. Mesh resolution at the boundaries varies between 0.015 and $0.02°^2$ and therefore was equal to or finer than the mesh resolution of mesh A at the boundaries.

For all model runs an input was included for the River Severn at the most inland limit of the model domain. The River Severn is the longest river in the UK and hence has a considerable discharge rate. The mean annual discharge rate of 107 m$^3$/s at the lowest river gauge on the River Severn (CEH, 2014) was applied to the model.

Sediment data is interpolated into a regular grid covering the model domain from a BGS dataset (British Geological Survey, 2013) using the Matlab griddata function with natural neighbour interpolation. A close up of the dataset and interpolation to model grid in the region of interest is shown in Fig. 5. There were sediment sampling limitations over the sandbanks, however comparison with datasets reported by Pattiaratchi and Collins (1987), Schmitt (2006) and Schmitt and Mitchell (2014) give confidence to the sediment grain size values utilised in this model. At the Helwick Bank, interpolation of the BGS data gave a median grain size of 0.35 mm over the entire bank area. This is very similar to the values reported by Schmitt and Mitchell (2014) who state that median grain size is 0.35 mm on the crest of the bank, 0.36 mm on the northern flank and 0.43 mm on the southern flank. At Scarweather Sands, Pattiaratchi and Collins (1987) reported that sediment is very well sorted fine to medium grained sand with mean grain sizes between Φ 1.6 and Φ 2.3 (0.2–0.32 mm) which gets finer towards the crest of the bank. In the BGS dataset, grain size values at Scarweather range from 0.2 to 0.4 mm. Schmitt (2006) reported, based on high spatial resolution sampling, that on the Nash sandbank median grain size varies from 0.2 to 0.5 mm (average $d_{50} = 0.35$) and that coarser sand and gravel is measured away from the sandbank.



Fig. 10. Residual currents at the Nash Bank for A) neap astronomical forcing, B) spring astronomical forcing, C) neap storm and surge forcing and D) spring storm and surge forcing.

The more sparsely sampled BGS data available to this work shows a similar pattern with median grainsize of 0.35 mm over the Nash Bank and coarse material further offshore and in the Nash passage.
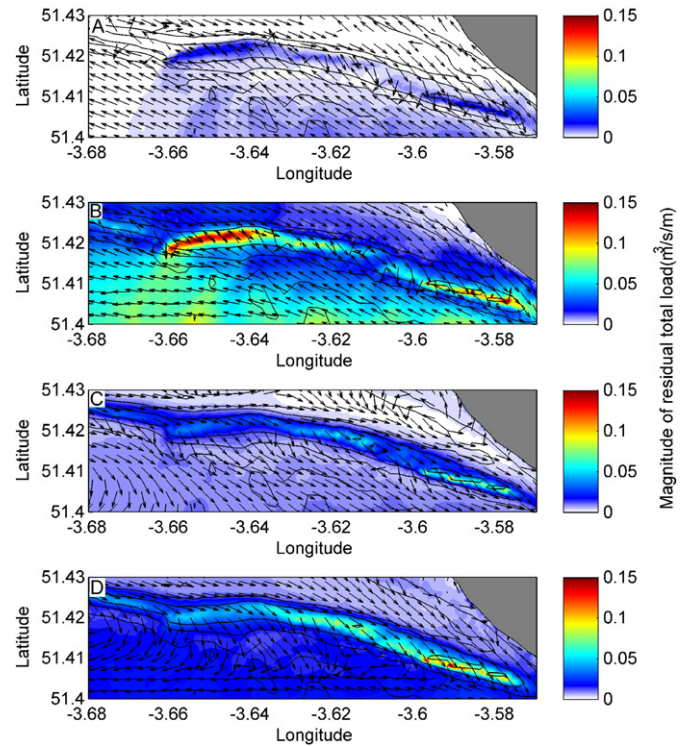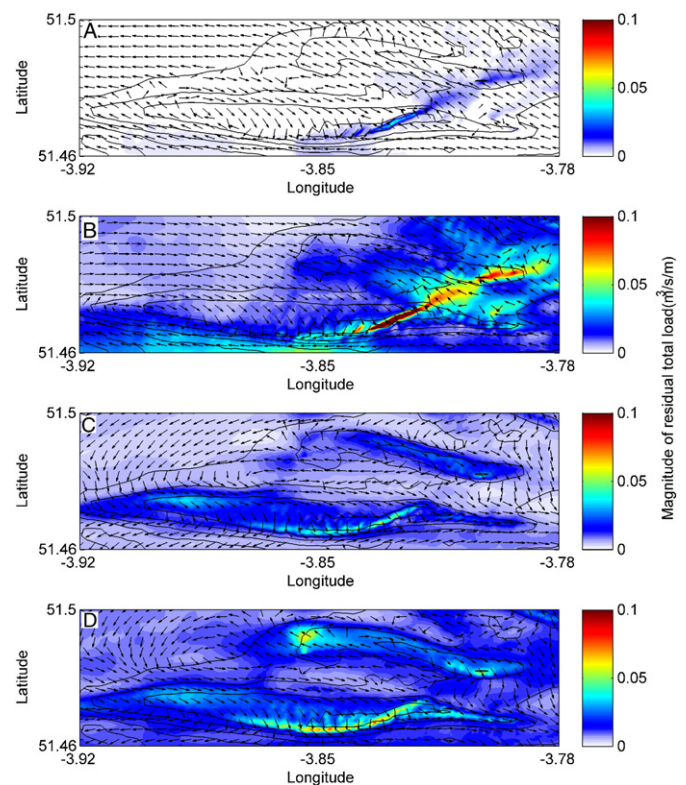


Fig. 11. Residual currents at the Scarweather Bank for A) neap astronomical forcing, B) spring astronomical forcing, C) neap storm and surge forcing and D) spring storm and surge forcing.

### 4.4. Model validation

Water level validation was conducted for two tide gauges at Mumbles and Ilfracombe. Validation of wave parameters was conducted at the Scarweather ($H_s$, $T_p$, *Direction*) and Turbot Bank ($H_s$, $T_z$) wave buoys. The locations of the Mumbles tide gauge and Scarweather wave buoy are shown in Fig. 1. The other two validation points are outside of the map extent. The Turbot Bank buoy is located further west at 51.603 N, 5.1 W. The Ilfracombe tide gauge is on the southern side of the Bristol Channel (51.21 N, 4.11 W).

Measured and modelled wave parameters are shown in Fig. 6 for the spring tide storm event. Parameters at Scarweather Sands are shown on the left hand side and Turbot Bank on the right. Directional information isn't shown for the Turbot Bank buoy because the buoy is non-directional. Correlation and error metrics for these buoys for both the spring and neap events are shown in Table 1. The $r^2$ value is significant at or above the 95% threshold for all parameters. For both buoys, the wave height is largely well replicated. The timing of the storm event is correct but the magnitude of the storm peak is under-represented; this is the same for the neap event (not shown). At both buoy locations, the values of the modelled period are similar to the measured values. For the wave buoy at Scarweather Sands, there are two episodes of short duration when the modelled wave period drops while the measured period remains constant. For other similar occurrences of reduction in peak period both modelled and measured periods are in agreement. The drops in wave period are semi-diurnal and it is postulated are caused by wave–current interaction. These drops in period are not evident for the Turbot Bank buoy in either measured or modelled data and thus the period is better modelled at this location. This is

evident both visually and in the error metrics (Table 1). The direction is less well modelled with a bias of about 10°.

Measured and modelled water levels are shown in Fig. 7. Visually, the model is performing adequately but there is an observable lag between model and measured data. The lag is approximately 30 min. Table 2 provides $r^2$ and RMSE values for Mumbles and Ilfracombe on spring and neap tides. It is interesting to note that the values are the same for the two different sites. The RMSE values are not that good due to the observed lag. However, removing the lag in the data improves the accuracy: the RMSE reduces to ~0.3 m and the $r^2$ values exceed 0.99. Given the locations of the tide gauges in shallow and complex (harbour) regions, this model performance is considered good.

## 5. Results

The results are split into three sections: model results for wave and hydrodynamic conditions are presented; the resulting residual sediment transport patterns are shown before the bed level changes and volume changes are compared. For both the spring and neap case, with and without storm and surge, the two tidal cycles covering the peak of the storm and surge are considered.

### 5.1. Wave and hydrodynamic results

Fig. 8 shows a spatial plot of the mean and maximum wave heights for the neap storm event in the left hand panels and differences between the neap and spring storm events in the right hand panels. Wave heights, both mean and maximum values are greatest in the west and reduce towards the east. This means that the Helwick Bank
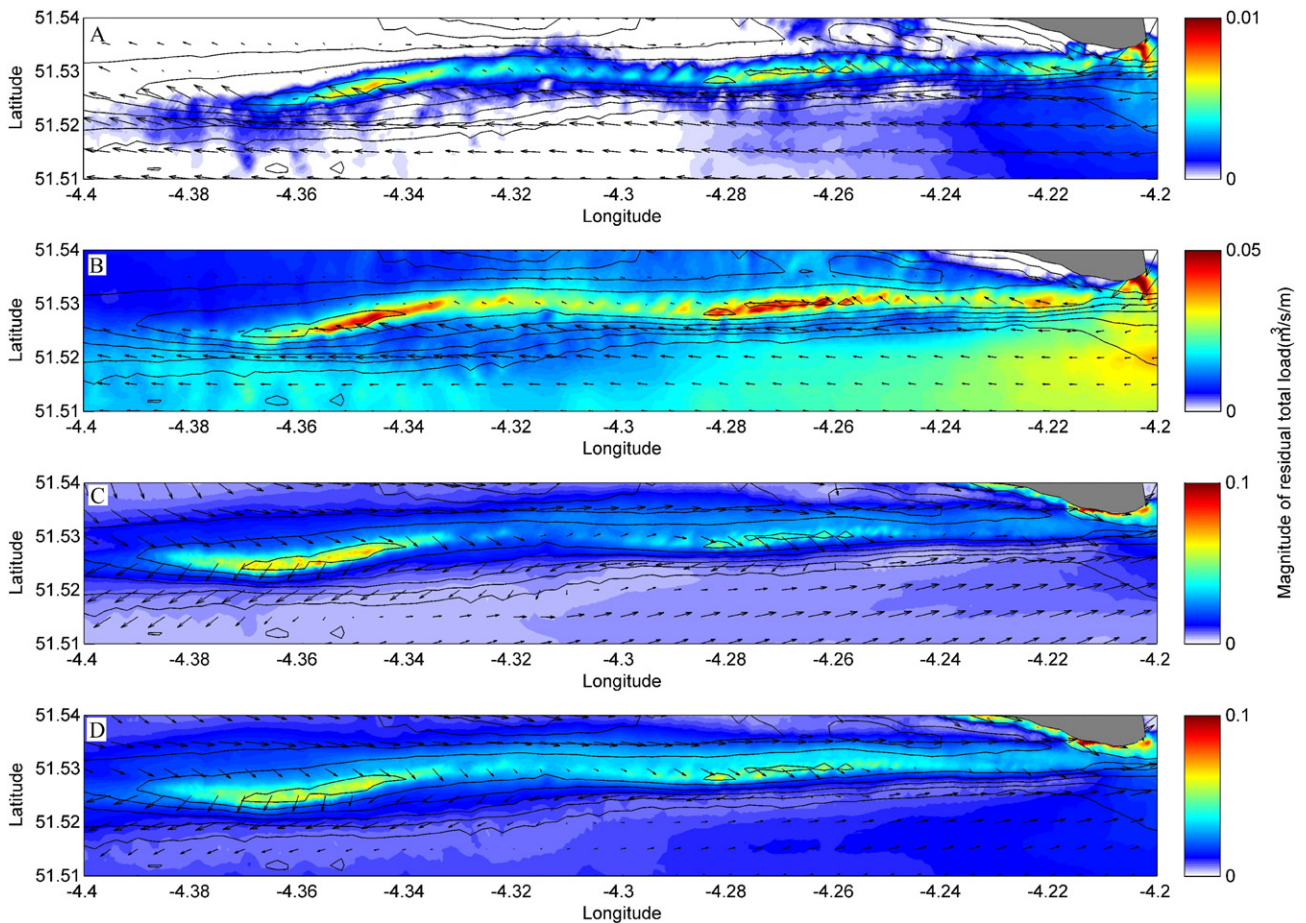


**Fig. 12.** Bedload residuals for the Helwick Bank. Vectors indicate direction and colour magnitude. A) Neap astronomical; B) spring astronomical; C) neap storm and surge; and D) spring storm and surge.
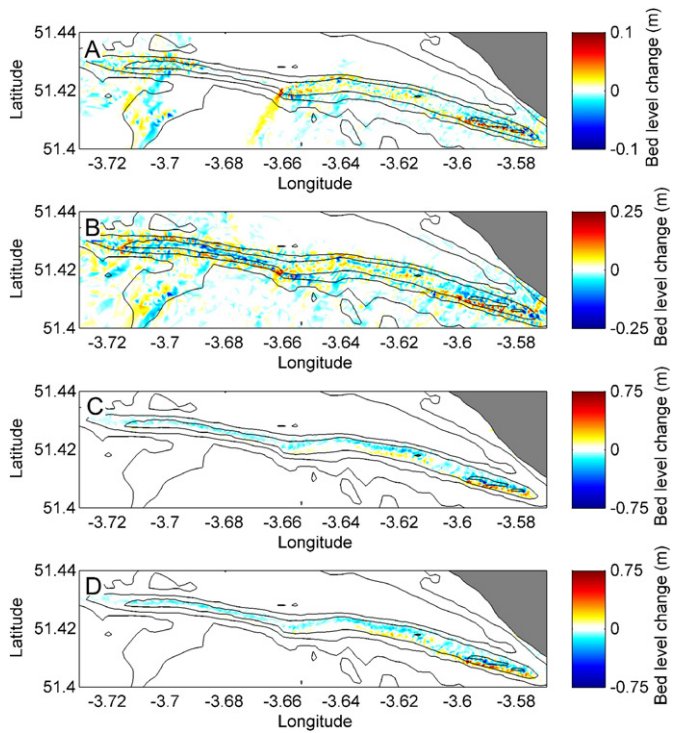
Fig. 13. Bed level changes for the four cases at Nash Bank: A) neap astronomical; B) spring astronomical; C) neap storm and surge; and D) spring storm and surge. Black lines indicate bathymetric contours and colour shading the bed level change.

experiences the greatest wave energy and the Nash Bank the least with Scarweather being between the two. For the mean wave height, wave heights are greater over most of the area of interest for the spring tide event apart from over the crest of the Scarweather and Nash sandbanks. The difference is small, being less than 0.2 m over most of the domain. The higher mean wave height over the crests for the neap tide event is due to greater water depths at low tide leading to lesser depth limited breaking. Maximum wave heights are greater over all three sandbanks for the spring tide event.

Fig. 9 shows maximum current speeds for the four tested cases. Current speeds from the astronomical runs increase from west to east. Peak currents are about 0.75 m s$^{-1}$ greater for the spring astronomic tide compared to the neap astronomic tide over the three sandbanks. For the astronomical forcing, peak currents at the sandbanks increase from Helwick in the west to Nash in the east. When wave and surge is included the patterns of maximum current alter with greatest currents over the sandbanks. The westernmost bank, Helwick, has the greatest current speed and this speed is similar for the neap and spring tide events. Maximum current speeds over the sandbanks when waves are included reduce from west to east. The reduction in current speed over the bank is greater for the neap tide compared to the spring tide. Maximum current speeds for the wave and surge case are more similar to the astronomical case for the Nash Bank (furthest east).

The results from this section indicate that the Helwick Bank is more likely to be wave dominated whereas the Nash Bank is more likely to undergo greater influence from tidal forcing.

### 5.2. Residual sediment transport pathways

In this section residual sediment transport pathways are presented. In all cases the figures show residual transport directions as vectors and the magnitude of the residual as colour shading. Contour lines show the model bathymetry.

Fig. 10 shows the bed load residuals for the Nash Bank for the different tests. Note that for clarity of figure the westernmost section of the

bank is not shown. For the neap astronomical tide residual total load pathways are in a clockwise direction around the bank. For the eastern portion of the bank pathways over the crest are from north to south and for the western portion pathways over the crest are from south to north. The neap storm and surge event shows the residual gyre is disrupted with residual transport pathways from west to east (up-estuary) for both sides of the sandbank and much of the wider area. Transport pathways are from north to south over the crest of the bank. The east to west portion of the residual gyre is observable on the westernmost section of the bank for the spring tide storm and surge event. There is also east to west residuals further offshore. Unlike the astronomical tide cases, transport over the crest is from north to south along the entire crest.

Magnitude of the residual transport is greatest over the crest of the bank. The magnitude is greatest for the spring astronomical tide case. For the storm and surge cases the magnitude is greatest on the eastern (shallowest) end of the bank where wave action is more dominant. For the astronomical cases magnitude of residual is greatest at either end of the bank.

Fig. 11 shows the same set of figures for Scarweather Sands. For the neap tide case, there is a clockwise gyre for the main sandbank and less defined patterns for the two associated sandbanks. Residual pathways are from north to south on the western, wider section of the crest and from south to north on the eastern narrower section of the crest. In general, away from the banks the residual total load transport is in an east to west direction. To the north of the sandbanks this is in a North Westerly direction, following the Swansea Bay coastline. For the spring astronomical case, similar patterns are evident. However, the residual
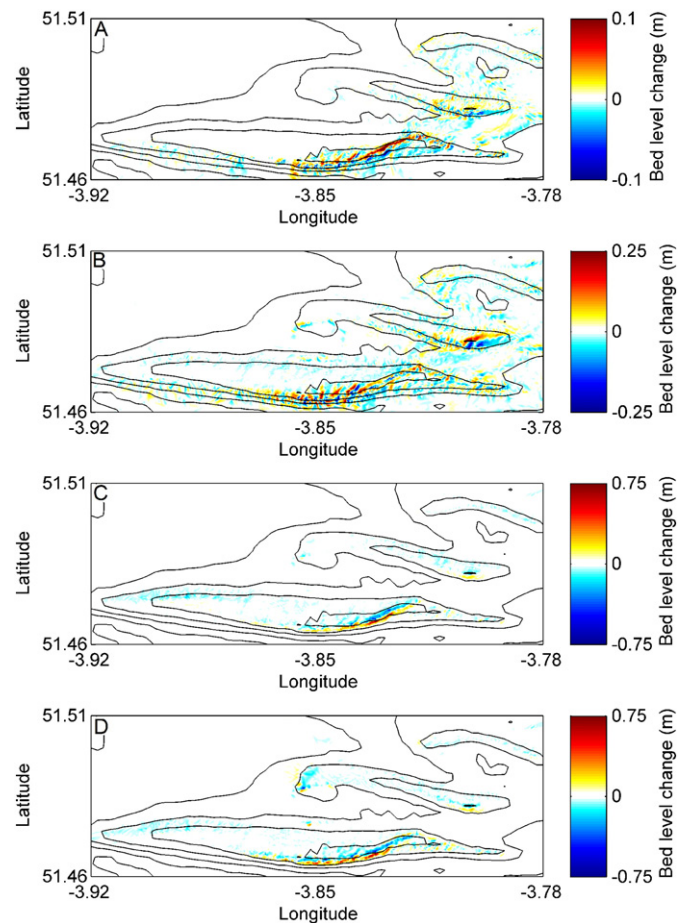


Fig. 14. Bed level changes for the four cases at Scarweather Sands: A) neap astronomical; B) spring astronomical; C) neap storm and surge; and D) spring storm and surge. Black lines indicate bathymetric contours and colour shading the bed level change.

gyre round the main bank is better defined and there are similar clockwise gyres around the two subsidiary banks. There is a greater convergence of pathways on the eastern half of the crest (pathways directed onto the crests from both northern and southern flanks).

For the neap storm and surge event residual transport pathways are directed towards the bank from the north. Residual pathways over the main bank are from east to west. There is still a small residual gyre which is only over the western portion of the bank. On the eastern (shallower) portion transport is from west to east on both flanks. Over the crest there is a southward component to the residual pathways. The same pattern is evident for the spring storm and surge event although there is not the same transport directed towards the bank from the north.

Fig. 12 shows the residual total load transport patterns for the Helwick Bank. Note that the variation in values between the different scenarios mean that colour maps span different ranges for the different sub-plots. For the neap astronomical tide there is a clockwise residual around the bank. The west to east residual is confined to the northern flank, whereas the east to west residual to the south covers a much larger area and extends to the south of the bank. The residual over the crest of the bank is towards the north west. The same pattern is shown for the spring astronomical tide.

For the both the spring and neap tide storm and surge events there is still a clockwise residual however the residual over the crest of the bank is directed towards the south east. The westward directed residual on the southern flank is confined to the flank itself with eastward residual pathways further south.

Magnitude of residual is again greatest over the crest for all cases. For the storm conditions this is focussed on the western, most wave exposed, end of the bank, whereas the astronomical residuals are similar along the entire crest. Spring and neap storm case residuals are similar

in magnitude. Maximum residual magnitudes are 10 times less for the neap astronomical case and slightly less for the spring astronomical case.

### 5.3. Bed level and volume change

Fig. 13 presents bed level change for the four test cases at the Nash Bank. For all plots of bed level change, it should be noted that scales are not consistent between sub-plots in order to best display the modelled changes. For the Nash sandbank, patterns of bed level change are similar for all four test cases: there is accretion on the southern flank and erosion on the northern flank. This is focussed on the eastern end of the sandbank. The magnitude of change differs however. Changes are greater for the spring astronomical tide case compared to the neap astronomical tide case, and over the areas of defined change this difference is of the order 0.1 m. For the two storm cases, the magnitude and shape of change is similar. The neap tide event shows greater change over the crest while there is greater change on the spring tide over the southern flank. It is suggested that the similarity in direction of change is due to the fact that despite residual transport pathways changing for the storm cases, over the eastern end of the bank they are always from north to south.

Fig. 14 presents the same for Scarweather Sands. The neap and spring astronomical cases show similar patterns with accretion on the north-western side and accretion on the south eastern side of the crest of the main sandbank. There is similar change over the crest of the secondary sandbank. Maximum bed level change approaches 0.25 m. The change over the spring tide is greater in magnitude (at most 0.15 m greater) and spread over a larger area.

Changes over the storm events are similar for both spring and neap tides. Changes are largely constrained to the sandbank crests. For both
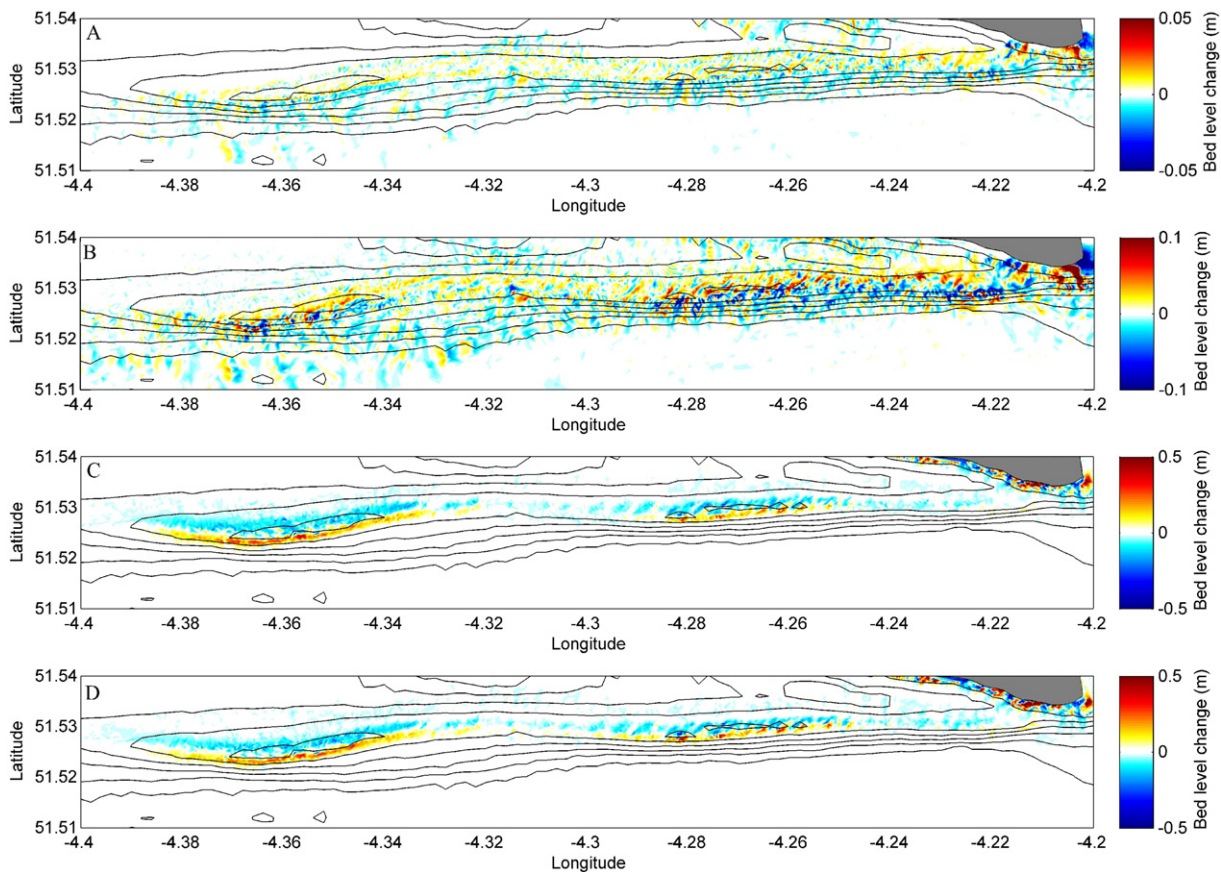


**Fig. 15.** Bed level changes for the four cases at Helwick Bank: A) neap astronomical; B) spring astronomical; C) neap storm and surge; and D) spring storm and surge. Black lines indicate bathymetric contours and colour shading the bed level change.

the spring and neap storm events, accretion occurs on the south-eastern flank and erosion on the north western flank. This is the opposite direction of change to the tide only events, although the locations of change are not identical. Maximum bed level change approaches 0.75 m for both cases. The relative impact of the storm is greater for the neap tide event with changes being 5 times greater than the tide only change compared to 2 times greater for the spring tide event.

The Helwick Bank (Fig. 15) is the furthest west of the sandbanks: it is more exposed to wave conditions but tidal currents are lower. For the neap astronomical case, changes are small, being less than 0.05 m. There is slight accretion on the northern crest of the bank and slight erosion on the southern flank. For the spring astronomical case the change is double that of the neap tide case: bed level changes are around 0.1 m. There is erosion on the southern flank and accretion on the crest and northern flank. The changes over the storm events are largely constrained to the crest of the sandbank, in depths less than 15 m, and the patterns are more defined. The change is the opposite direction to the tide only case with accretion on the southern side of the crest and erosion on the northern side. Patterns of change are spread over a slightly wider area for the neap tide event. In both cases magnitude of maximum bed level change is around 0.4 m.

The bed level changes and sediment transport pathways are summarised in a conceptual fashion in Fig. 16. Distinction is made between tidal and storm driven conditions but not spring and neap cases. Tidally driven sediment transport pathways are shown as arrows of orange outline while storm driven sediment transport is shown as black hatched arrows. Bed level changes for the tidal scenarios are shown as solid colours with blue for areas of erosion and yellow for areas of accretion. For Scarweather Sands and the Helwick Bank, where storm driven changes oppose tidally driven changes, storm driven changes are marked with cross-hatched areas: blue for erosion and red for accretion. For all storm cases, sediment transport pathways are altered from the tide alone case and areas of maximum change are focussed on the sandbank crest. For the Nash Bank the direction is the same as the tidal case whereas for the other two cases the direction of change over the crest of the bank is opposite.

Fig. 17 presents relative volume change for the three banks over the 4 test cases. For reference, absolute volume changes are presented in Table 3. Volume change is calculated for areas of the bank shallower than −15 m MSL for the Scarweather and Nash Banks and for areas shallower than −20 m MSL for the Helwick Bank which has a deeper crest. Volumes are expressed as percentage changes of the total volume to allow better comparison between sandbanks. In general changes are small being less than 1% for the storm events and less than 0.03% for the astronomical changes. For all cases the storm events lead to a reduction in sandbank volume; for the Helwick and Nash Banks the magnitude of the reduction is similar and for both banks the neap tide event shows slightly greater reduction.

## 6. Discussion

This work has used a numerical model, MIKE3, to investigate storm impacts on the morpho-dynamics of offshore sandbanks. The model was validated against tide gauges and wave buoys close to the study area. Validation showed a good agreement between modelled and measured data. There was a lag of 1/2 h between measured and modelled data, this could be due to inaccuracies in the bathymetry or bed resistance of the wider domain, particularly in the upper limits of the Severn Estuary. Equally the location of tidal gauges in shallow water and complex topography means that the model will not accurately represent the local area. While in general the wave model was observed to perform well, there was an under representation of the peak storm wave heights. Such under representation has been observed in various other model studies for a range of locations worldwide (Akpinar et al., 2012; Bidlot et al., 2002; Cardone et al., 1996; Sandhya et al., 2014). The missing peak is of the same duration as the time step between successive

wind field inputs and therefore some under-representation could be due to insufficient wind data, as has previously been suggested (Sandhya et al., 2014). Spatial resolution of wind data, too low peak wind speeds and lack of consideration of gustiness can also contribute to inaccuracies in modelled wave height (Cavaleri, 2009). The model formulation is also likely to lead to under prediction of storm wave heights due to inaccurate formulations for non-linear energy transfer and for whitecapping (Cavaleri, 2009). Typically formulations of non-linear interactions lead to over-distribution of energy in frequency and direction, reducing the peak wave height (Cavaleri, 2009).

The model was only partially coupled for simulations including waves due to computational restrictions. While the hydrodynamic model and the sediment transport/morphology model were on-line coupled, the wave forcing was off-line. This means that the hydrodynamic forcing and sediment transport adapts to the changing morphology but the wave forcing does not. Wave forcing consists of radiation stresses fed into the hydrodynamic model and wave parameters directly to the sediment transport model. For the Helwick Bank, maximum bed level changes are less than 5% of the mean water depth at the location of maximum change and the bank is continually submerged meaning that the lack of fully coupled wave forcing is unlikely to make a significant difference to results. For the Nash and Scarweather Banks, maximum bed level changes correspond to 15% of the mean water depth and the areas are emergent at low tide for the spring case, therefore there is greater likelihood of modelling errors. However, it has been suggested that uncoupled models are adequate for comparative studies and for assessing the difference between storm, background wave and tidal forcing (de Vriend et al., 1993). Therefore it is believed that the results presented here are still relevant, despite the likelihood of some deviations from actuality.

This work corroborates findings by Pattiaratchi and Collins (1988), who analysed Scarweather Sands and found that residual sediment transport occurs in a clockwise direction for astronomical forcing. This
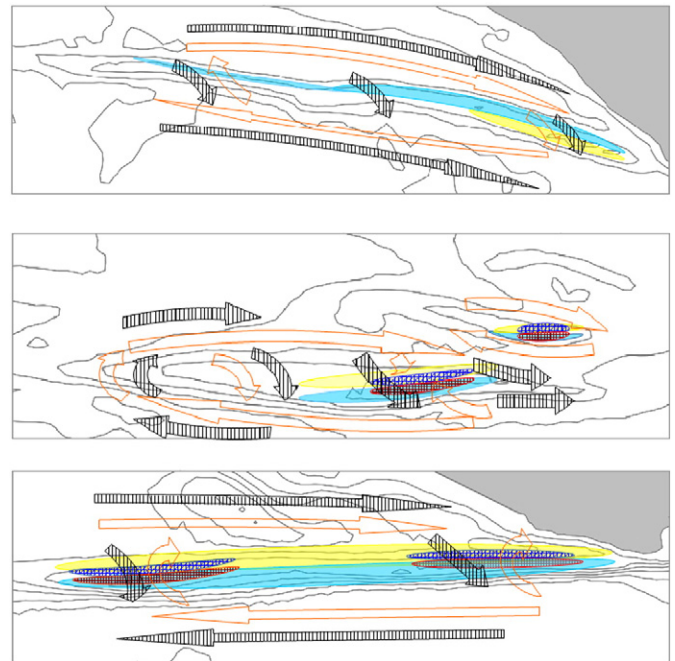


Fig. 16. A conceptual diagram showing sediment transport pathways and bed level change for the three sandbanks: Nash (upper panel); Scarweather (middle panel) and Helwick (bottom panel). Tidally driven sediment transport pathways are shown as arrows of orange outline; storm driven shown as black hatched arrows. Bed level changes for the tidal scenarios are shown as solid colours with blue for areas of erosion and yellow for areas of accretion. Storm driven changes are marked with cross-hatched areas: blue for erosion and red for accretion.
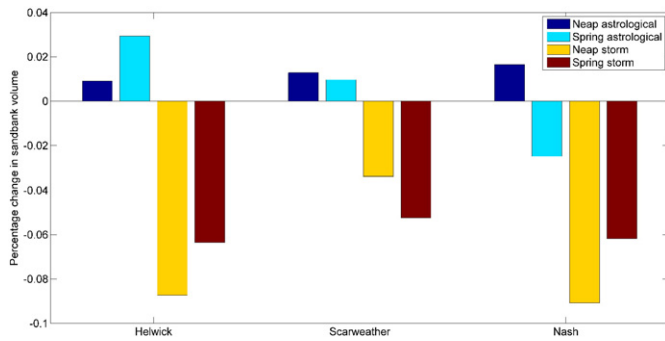
**Fig. 17.** Relative volume changes as percentages of total bank volume for the three banks and the four different cases.

is the case for all tested sandbanks at both spring and neap tides. Under storm conditions these residuals are altered. More recently, repeat multibeam and single-beam surveys have been conducted at the Nash and Helwick Banks by Schmitt (2006), Schmitt and Mitchell (2014), Scmitt et al. (2007), and Schmitt et al. (2008), focussing on the morphology and dynamics of sand waves on the banks to infer sediment transport. Sand dunes have been found on the flanks of the Helwick Bank, which are classified as very large, based on the designation of Ashley (1990). These have lee slopes orientated to the east on the northern flank and to the west on the southern flank which indicates clockwise residual sediment transport (Schmitt and Mitchell, 2014). To the east of the Helwick Bank, between the bank and the land are fields of sand dunes with crests running from southwest to northeast. Their shape indicates south-eastward transport of sediment (Scmitt et al., 2007). The results are derived from dune morphology for sediment transport direction support and give confidence to the numerically modelled sediment transport pathways presented in this paper for the Helwick Bank. Maps of erosion and accretion for the Helwick Bank over one year (Schmitt and Mitchell, 2014) show broadly similar patterns of change as the results presented here for the astronomical cases. The resolution of the results presented in Schmitt and Mitchell (2014) is insufficient to show the storm scale changes which are shown to be highly focussed on the crest in the results contained here. An interesting phenomenon was observed at the Helwick Bank where sand dunes on either flank were connected over the crest, despite the dunes on each flank travelling in the opposite directions. It is postulated (Schmitt and Mitchell, 2014) that wave action causes re-connection between successive dunes. They report that wave induced currents exceed tidal currents for 25% of the time on the Northern flank and for 50% of the time on the crest, wave direction is parallel to the line of the sand dune crests and hence promotes dune parallel sand transport and crest re-connection. Less detailed morphological information was available at the Nash Bank, nevertheless Schmitt (2006) drew some conclusions about the Nash Bank: analysis of dune morphology and migration showed a clockwise residual circulation around the bank; low amplitude and long wavelength sand dunes on the crestal escarpment indicate the importance of wave breaking to sediment transport over the crest; and consideration of bathymetric variation suggested a relatively constant erosion of the bank. These findings support the results of the current numerical modelling; in particular, despite being

the most tidally dominated bank tested, wave effects are still important at Nash Bank.

Bed level changes over the crest of the banks for storm and surge events are greater in magnitude and in the opposite direction to the astronomically forced change for the Helwick and Scarweather Banks. It is therefore postulated that episodic storm conditions help to maintain the location and shape of the crest of these sandbanks against the long term background impact of astronomically forced changes and could be a factor in sandbank maintenance for wave exposed environments.

Bed level changes at the Nash Bank are in the same direction for both astronomical and storm events. This is due to similarities in the residual sediment transport pathways between both cases and may be related to the increased tidal currents and reduced wave heights relative to the other banks. For the Nash Bank tidal forcing is dominant with wave action enhancing transport.

Erosion and deposition of sediment under storm conditions can affect grain sizes with finer grain sizes removed from the crest and deposited in more sheltered areas (Houthuys et al., 1994). Model outputs are not available to test this, however it would suggest a re-distribution of finer material towards the flanks. Pattiaratchi and Collins (1987) found that grain sizes became increasingly fine towards the crest at Scarweather and therefore any storm induced coarsening of crestal sediment must be matched by transport of finer material to the crest under low energy conditions. One aspect that has not been considered is the rates of volume change under low energy wave conditions. Under such conditions wave action may enhance sediment mobility without altering pathways from the tide-only cases and hence rates of volume increase on the banks may be greater than the tested cases under some conditions.

Lewis et al. (2014) have found that the volume of the Nash Bank increases in years with numerous storms. For the storms studied here all banks are reduced in volume over storm events. For both the Nash and Helwick Banks volume changes are greater for the neap tide event whereas for the Scarweather Sands bank reductions are greater for the spring tide event. The Nash and Helwick Banks are more similar morphologically, whereas the Scarweather Bank is further offshore from the coast, with additional secondary banks. Under neap tide conditions there is a residual sand transport towards the bank from the north which may provide a sediment supply that reduces the erosion under neap storm and surge conditions and leads to this disparity.

For the Helwick Bank (lowest tidal currents) there is a volume increase for both astronomical cases with greater increase for the spring tide; for the Scarweather Bank, while there are still increases in volume, the increase is less and the neap tide increase is greater; for the Nash Bank (greatest tidal currents) there is an increase in volume for the neap astronomical case but a reduction in volume for the spring astronomical case. The relative increase in volume for the neap tide case increases from west to east (increasing maximum current speed and also tidal range). Given that there are clockwise residual gyres for all banks under spring and neap astronomical forcing, it is perhaps unsurprising that volume changes scale with current speeds and tidal range. There is a large difference between spring and neap tidal ranges in the area which may account for the difference between spring and neap tidal changes.

## 7. Conclusions

This work provides insights into a previously under-studied area: the impact of extreme storms on offshore sandbanks. Developing understanding of storm impacts is important for the proper management of these environments and allows understanding of the relative impact of both climate change and industrial activity. Here, three sandbanks in the same area are studied which have differences in relative wave and tidal forcing and in morphological settings. Storms alter residual currents over the sandbanks, altering or removing the tidally forced clockwise residual gyre. For the two more wave dominated banks

**Table 3**
Volume changes for the three sandbanks under different conditions ($\times 10^3$ m$^3$).

|              | Neap astronomical | Spring astronomical | Neap storm | Spring storm |
| ------------ | ----------------- | ------------------- | ---------- | ------------ |
| Helwick      | 636               | 2060                | −6115      | −4452        |
| Scarweather  | 2520              | 1890                | −6626      | −10,265      |
| Nash         | 720               | −1082               | −3941      | −2684        |

storm conditions act to force opposite patterns of bed level change over the crest of the bank compared to astronomically forced change but with greater magnitude. For the more tidally dominated bank patterns of bed level change are similar for both storm and astronomical conditions.

There are clear links between tidal conditions at the banks and astronomically forced volume change: as maximum tidal currents (and tidal range) increase the magnitude of volume increase for neap tide increases while the volume change at spring tide goes from positive to negative. Storm induced volume changes are similar for the eastern-most and western-most banks, which are morphologically similar, and different for the central bank which is different morphologically. This suggests that under storm conditions morphology and setting is more important than relative contributions of wave and tidal forcing.

## Acknowledgements

## References

Ahmadian, R., Falconer, R.A., 2012. Assessment of array shape of tidal stream turbines on hydro-environmental impacts and power output. Renew. Energy 44, 318–327.

Ahmadian, R., Falconer, R.A., Bockelmann-Evans, B., 2012. Far-field modelling of the hydro-environmental impact of tidal stream turbines. Renew. Energy 38, 107–116.

Akpinar, A., van Vledder, G.P., Komurcu, M.I., Ozger, M., 2012. Evaluation of the numerical wave model (SWAN) for wave simulation in the Black Sea. Cont. Shelf Res. 50-51, 80–99.

Anderson, O.B., 1995. Global ocean tides from ERS-1 and TOPEX/POSEIDON altimetry. J. Geophys. Res. 100, 25249–25259.

Anderson, O.B., 1999. Shallow water tides on the northwest European shelf from TOPEX/POSEIDON altimetry. J. Geophys. Res. 104, 7729–7741.

Ashley, G.M., 1990. Classification of large-scale subaqueous bedforms: a new look at an old problem. J. Sediment. Petrol. 60, 160–172.

Atalah, J., Fitch, J., Coughlan, J., Chopelet, J., Coscia, I., Farrell, E., 2013. Diversity of demersal and megafaunal assemblages inhabiting sandbanks of the Irish Sea. Mar. Biodivers. 43, 121–132.

Bastos, A.C., Kenyon, N.H., Collins, M., 2002. Sedimentary processes, bedforms and facies, associated with a coastal, headland: Portland Bill, Southern UK. Mar. Geol. 187, 235–258.

Bastos, A.C., Paphitis, D., Collins, M.B., 2004. Short-term dynamics and maintenance processes of headland-associated sandbanks: Shambles Bank, English Channel, UK. Estuar. Coast. Shelf Sci. 59, 33–47.

Berthot, A., Pattiaratchi, C., 2005. Maintenance of headland-associated linear sandbanks: modelling the secondary flows and sediment transport. Ocean Dyn. 55, 526–540.

Berthot, A., Pattiaratchi, C., 2006. Mechanisms for the formation of headland-associated linear sandbanks. Cont. Shelf Res. 26, 987–1004.

Bidlot, J.R., Holmes, D.J., Wittmann, P.A., Lalbeharry, R., Chen, H.S., 2002. Intercomparison of the performance of operational ocean wave forecasting systems with buoy data. Weather Forecast. 17, 287–310.

British Geological Survey, 2013. BGS legacy particle size analysis uncontrolled data export.

Cardone, V.J., Jensen, R.E., Resio, D.T., Swail, V.R., Cox, A.T., 1996. Evaluation of contemporary ocean wave models in rare extreme events: the "Halloween storm" of October 1991 and the "Storm of the Century" of March 1993. J. Atmos. Ocean. Technol. 13, 198–230.

Cavaleri, L., 2009. Wave modeling—missing the peaks. J. Phys. Oceanogr. 39, 2757–2778.

CEH, 2014. National River Flow Archive.

Collins, M.B., Shimwell, S.J., Gao, S., Powell, H., Hewitson, C., Taylor, J.A., 1995. Water and sediment movement in the vicinity of linear sandbanks — the Norfolk Banks, Southern North Sea. Mar. Geol. 123, 125–142.

Coughlan, C., Vincent, C.E., Dolphin, T.J., Rees, J.M., 2007. Effects of tidal stage on the wave climate inshore of a sandbank. J. Coast. Res. 751-756.

Dafforn, K.A., Mayer-Pinto, M., Morris, R.L., Waltham, N.J., 2015. Application of management tools to integrate ecological principles with the design of marine infrastructure. J. Environ. Manag. 158, 61–73.

de Vriend, H.J., Zyserman, J., Nicholson, J., Roelvink, J.A., Péchon, P., Southgate, H.N., 1993. Medium-term 2DH coastal area modelling. Coast. Eng. 21, 193–224.

Dee, D.P., Uppala, S.M., Simmons, A.J., Berrisford, P., Poli, P., Kobayashi, S., Andrae, U., Balmaseda, M.A., Balsamo, G., Bauer, P., Bechtold, P., Beljaars, A.C.M., van de Berg, L., Bidlot, J., Bormann, N., Delsol, C., Dragani, R., Fuentes, M., Geer, A.J., Haimberger, L., Healy, S.B., Hersbach, H., Hólm, E.V., Isaksen, L., Kållberg, P., Köhler, M., Matricardi, M., McNally, A.P., Monge-Sanz, B.M., Morcrette, J.J., Park, B.K., Peubey, C., de Rosnay, P., Tavolato, C., Thépaut, J.N., Vitart, F., 2011. The ERA-interim reanalysis: configuration and performance of the data assimilation system. Q. J. R. Meteorol. Soc. 137, 553–597.

DHI, 2012a. MIKE 3 Flow Model FM — Hydrodynamic Module — User Guide. DHI, p. 130.

DHI, 2012b. MIKE 21 and MIKE 3 Flow Model FM — Hydrodynamic and Transport Module — Scientific Documentation.

Dolphin, T.J., Vincent, C.E., Coughlan, C., Rees, J.M., 2007. Variability in sandbank behaviour at decadal and annual time-scales and implications for adjacent beaches. J. Coast. Res. 731–737.

Draper, L., 1991. Wave Climate Atlas of the British Isles. HMSO, London.

Englund, F., Fredsoe, J., 1976. A sediment transport model for straight alluvial channels. Nord. Hydrol. 7, 296–306.

Fairley, I., Ahmadian, R., Falconer, R.A., Willis, M.R., Masters, I., 2014. The effects of a Severn barrage on wave conditions in the Bristol Channel. Renew. Energy 68, 428–442.

Flather, R.A., 1987. Estimates of extreme conditions of tide and surge using a numerical model o the north-west European continental shelf. Estuar. Coast. Shelf Sci. 24, 69–93.

Fredsoe, J., Anderson, O.H., Silberg, S., 1985. Distribution of suspended sediment in large waves. J. Waterw. Port Coast. Ocean Eng. 3, 1041–1059.

Giardino, A., Van den Eynde, D., Monbaliu, J., 2010. Wave effects on the morphodynamic ecolution of an offshore sand bank. J. Coast. Res. SI 51, 127–140.

Hall, J.K., 2006. GEBCO centennial special issue — charting the secret world of the ocean floor: the GEBCO project 1903–2003. Mar. Geophys. Res. 27, 1–5.

Horrillo-Caraballo, J.M., Reeve, D.E., 2008. Morphodynamic behaviour of a nearshore sandbank system: the Great Yarmouth Sandbanks, UK. Mar. Geol. 254, 91–106.

Houthuys, R., Trentesaux, A., Dewolf, P., 1994. Storm influences on a tidal sandbanks surface (Middlekerke Bank, Southern North Sea). Mar. Geol. 121, 23–41.

HSE, 2001. Wind and Wave Frequency Distributions for Sites Around the British Isles. Fugro GEOS.

Idier, D., Hommess, S., Briere, C., Roos, P.C., Walstra, D.J.R., Knaapen, M.A.F., Hulscher, S.J.M.H., 2010. Morphodynamic models used to study the impact of offshore aggregate extraction: a review. J. Coast. Res. 39-52.

Iliffe, J.C., Ziebart, M.K., Turner, J.F., Talbot, A.J., Lessnoff, A.P., 2013. Accuracy of vertical datum surfaces in coastal and offshore zones. Surv. Rev. 45, 254–262.

Kaiser, M.J., Bergmann, M., Hinz, H., Galanidi, M., Shucksmith, R., Rees, E.I.S., Darbyshire, T., Ramsay, K., 2004. Demersal fish and epifauna associated with sandbank habitats. Estuar. Coast. Shelf Sci. 60, 445–456.

Lewis, M.J., Neill, S.P., Elliott, A.J., 2014. Interannual variability of two offshore sand banks in a region of extreme tidal range. Journal of Coastal Research in press.

Lionello, P., Boldrin, U., Giorgi, F., 2008. Future changes in cyclone climatology over Europe as inferred from a regional climate simulation. Clim. Dyn. 30, 657–671.

Lowe, J.A., Gregory, J.M., 2005. The effects of climate change on storm surges around the United Kingdom. Philos. Trans. R. Soc. A Math. Phys. Eng. Sci. 363, 1313–1328.

Lowe, J.A., Gregory, J.M., Flather, R.A., 2001. Changes in the occurrence of storm surges around the United Kingdom under a future climate scenario using a dynamic storm surge model driven by Hadley Centre climate models. Clim. Dyn. 18, 179–188.

Neill, S.P., 2008. The role of Coriolis in sandbank formation due to a headland/island system. Estuar. Coast. Shelf Sci. 79, 419–428.

NTSLF, 2014. Highest & lowest predicted tides at Mumbles. (Available online: http://www.ntslf.org/tgi/portinfo?port=Mumbles).

Olbert, A.I., Dabrowski, T., Nash, S., Hartnett, M., 2012. Regional modelling of the 21st century climate changes in the Irish Sea. Cont. Shelf Res. 41, 48–60.

Park, H.B., Vincent, C.E., 2007. Evolution of Scroby Sands in the East Anglian coast, UK. J. Coast. Res. 868–873.

Pattiaratchi, C., Collins, M., 1987. Mechanisms for linear sandbank formation and maintenance, in realtion to dynamical oceanographic observations. Prog. Oceanogr. 19, 117–176.

Pattiaratchi, C., Collins, M.B., 1988. Wave influence of coastal sand transport paths in a tidally dominated environment. Ocean Shoreline Manag. 11, 49–465.

Phillips, M.R., 2008. Beach erosion and marine aggregate dredging: a question of evidence? Geogr. J. 174, 332–343.

Reeve, D., Li, B., Thurston, N., 2001. Eigenfunction analysis of decadal fluctuations in sandbank morphology at Gt Yarmouth. J. Coast. Res. 17, 371–382.

Sandhya, K.G., Nair, T.M.B., Bhaskaran, P.K., Sabique, L., Arun, N., Jeykumar, K., 2014. Wave forecasting system for operational use and its validation at coastal Puducherry, east coast of India. Ocean Eng. 80, 64–72.

Schmitt, T., 2006. Morphology and dynamics of headland connected sandbanks form high resolution bathymetric surveys: Helwick and Nash Sands, Bristol Channel, UK. Cardiff University, Cardiff, p. 260.

Schmitt, T., Mitchell, N.C., 2014. Dune-associated sand fluxes at the nearshore termination of a banner sand bank (Helwick Sands, Bristol Channel). Cont. Shelf Res. 76, 64–74.

Schmitt, T., Mitchell, N.C., Ramsay, A.T.S., 2008. Characterizing uncertainties for quantifying bathymetry change between time-separated multibeam echo-sounder surveys. Cont. Shelf Res. 28, 1166–1176.

Scmitt, T., Mitchell, N.C., Ramset, A.T.S., 2007. Use of swath bathymetry in the investigation of sand dune geometry and migration around a nearshore 'banner' tidal sandbank. In: Balson, P.S., Collins, M.B. (Eds.), Coastal and Shelf Seidment Transport, special publiaction, 274. Geological Society of London, pp. 53–64.

Smagorisky, J., 1963. General circulation experiment with the primitive equations. Mon. Weather Rev. 91, 99–164.

Sorenson, O.R., Kofoed-Hansen, H., Rugbjerg, M., Sorenson, L.S., 2004. A third-generation spectral wave model using an unstructured finite volume technique. In: Mckee-Smith, J. (Ed.), ICCE. World Scientific, Lisbon, pp. 894–906.

TLSB, 2014. (website: http://www.tidallagoonswanseabay.com/accessed 01/2015).

UKHO, 2014. (Data available online: https://www.gov.uk/inspire-portal-and-medin-bathymetry-data-archive-centre).

Uncles, R.J., 2010. Physical properties and processes in the Bristol Channel and Severn Estuary. Mar. Pollut. Bull. 61, 5–20.

Van de Meene, J.W.H., Van Rijn, L.C., 2000. The shoreface-connected ridges along the central Dutch coast — part 2: morphological modelling. Cont. Shelf Res. 20, 2325–2345.

Van Lancker, V.R.M., Bonne, W., Velegrakis, A.F., Collins, M.B., 2010. Aggregate extraction from tidal sandbanks: is dredging with nature an option? Introduction. J. Coast. Res. 53–61.

Van Rijn, L.C., 1984a. Sediment transport, part 1: bed load transport. J. Hydraul. Eng. 110, 1431–1456.

Van Rijn, L.C., 1984b. Sediment transport, part II: suspended load transport. J. Hydraul. Eng. 110, 1613–1641.

Vincent, C.E., Stolk, A., Porter, C.F.C., 1998. Sand suspension and transport on the Middelkerke Bank (southern North Sea) by storms and tidal currents. Mar. Geol. 150, 113–129.

Wang, S., McGrath, R., Hanafin, J., Lynch, P., Semmler, T., Nolan, P., 2008. The impact of climate change on storm surges over Irish waters. Ocean Model. 25, 83–94.

Xia, J.Q., Falconer, R.A., Lin, B.L., 2010. Hydrodynamic impact of a tidal barrage in the Severn Estuary, UK. Renew. Energy 35, 1455–1468.